Breast fibroblasts in both cancer and normal tissues induce phenotypic transformation of breast cancer stem cells: a preliminary study

Bixiao Wang[1], Chunfang Xi[1, 2], Mingwei Liu[3], Haichen Sun[4], Shuang Liu[4], Lei Song[3], and Hua Kang[1]

1. Department of General Surgery, Xuanwu Hospital, Capital Medical University, Beijing, China

2. Department of Breast Surgery, Shanxi Provincial People's Hospital, Taiyuan, Shanxi, China

3. State Key Laboratory of Proteomics, National Center for Protein Sciences, Beijing Proteome Research Center, Beijing, China

4. Surgery Lab, Xuanwu Hospital, Capital Medical University, Beijing, China

Abstract

Background. Breast cancer stem cells (BCSCs) are associated with the invasion of breast cancer. In recent years, studies have demonstrated different phenotypes among BCSCs. Furthermore, BCSCs of diverse phenotypes are present at different tumour sites and different histological stages. Fibroblasts are involved in the phenotypic transformation of BCSCs. Cancer-associated fibroblasts (CAFs) participate in the induction of epithelial-mesenchymal transition, thereby promoting the acquisition of stem cell characteristics, but little is known about the role of normal fibroblasts (NFs) in the phenotypic transformation of BCSCs or about the effect of CAFs and NFs on BCSC phenotypes.

Methods. Six pairs of primary CAFs and NFs were isolated from surgical samples of breast cancer patients and subjected to morphological, immunohistochemical, cell invasion and proteomics analyses. After establishing a cell culture system with conditioned medium from CAFs and NFs, we used the mammosphere formation assay to explore the effect of CAFs and NFs on the self-renewal ability of BCSCs. The effect of CAFs and NFs on the phenotypic differentiation of BCSCs was further analysed by flow cytometry and immunofluorescence.

Results. The isolated CAFs and NFs did not show significant differences in cell morphology or α-SMA expression, but cell invasion and proteomics analyses demonstrated heterogeneity among these fibroblasts. Both CAFs and NFs could promote the generation of BCSCs, but CAFs displayed a greater capacity for promoting mammosphere formation than NFs. Conditioned

41 medium from CAFs increased the proportion of ALDH1$^+$ BCSCs, but conditioned medium from

42 NFs was more likely to promote the generation of CD44$^+$CD24$^-$ BCSCs from MCF-7 cells.

43 **Discussion.** This study validated the heterogeneity among CAFs and NFs and expanded on the

44 conclusion that fibroblasts promote the generation of cancer stem cells. Our results particularly

45 emphasized the effect of NFs on the phenotypic transformation of BCSCs. In addition, this study

46 further highlighted the roles of CAFs and NFs in the induction of different phenotypes in BCSCs.

47

Introduction

49 Cancer stem cells are a subpopulation of cancer cells that are characterized by self-renewal and

50 multidirectional differentiation capabilities. Since breast cancer stem cells (BCSCs) were isolated

51 in 2003 and shown to exhibit strong tumourigenicity (Al-Hajj et al. 2003), a large number of

52 studies have described the use of CD44, CD24 and aldehyde dehydrogenase-1 (ALDH1) for the

53 identification of BCSCs (Chiotaki et al. 2016; Yang et al. 2017). These studies have shown that

54 BCSCs are associated with tumour progression such as recurrence, metastasis and treatment

55 resistance, and consequently contributed to the poor outcome of breast cancer. However, not all

56 BCSC markers are expressed in all breast cancer subtypes, and these markers may be limited to

57 particular subtypes or associated with invasive subtypes of breast cancer (Boesch et al. 2016). For

58 example, CD44$^+$CD24$^-$ BCSCs are abundant in triple-negative breast cancer (TNBC) (Bernardi et

59 al. 2012), and ALDH1$^+$ BCSCs are associated with the BRCA1 mutational status (Somasundaram

60 et al. 2016). In addition, these cell populations are enriched in primary tumour lesions after

61 radiotherapy and chemotherapy but are seldom associated with either disease-free or overall

62 survival (Li et al. 2008). However, ALDH1$^+$ BCSCs are associated with HER-2 overexpression

63 and loss of expression of oestrogen receptors and progesterone receptors (Ginestier et al. 2007),

64 and the presence of this population may be used as an independent predictor of breast cancer

65 prognosis (Mansour & Atwa 2015). These findings indicate that BCSCs may vary by cancer

66 subtype. Even for a particular breast cancer lesion, there may be differences in stem cell

67 phenotypes at different tumour sites and different histological stages (A & Lopes 2017). Therefore,

68 we hypothesize that a process of transformation is involved in the variation of BCSC phenotypes.

69

70 The tumour matrix or the tumour microenvironment can affect the biological behaviour of cancer

71 cells and plays an important role in the disease progression (Bussard et al. 2016). Fibroblasts are

72 the major cellular components in the tumour microenvironment, and fibroblasts that are activated

73 by cancer cells are called cancer-associated fibroblasts (CAFs). Many studies have shown that

74   CAFs play an important role in tumour formation, development, invasion, metastasis and

75   resistance to treatment by secreting exosomes or a variety of cytokines and factors that remodel

76   the extracellular matrix (Buchsbaum & Oh 2016; Erdogan & Webb 2017). CAFs are thus involved

77   in inducing epithelial-mesenchymal transition and can promote the acquisition of stemness in

78   breast cancer cells (Giannoni et al. 2010; Plaks et al. 2015). However, during the initial stages of

79   formation of primary or metastatic lesions, the tumour microenvironment mostly contains normal

80   fibroblasts (NFs). Some of these resting NFs can be activated due to inflammation, tissue damage,

81   chronic fibrosis and other processes to become normal activated fibroblasts (NAFs) (Darby et al.

82   2016). However, very little is known regarding the function of the two populations of fibroblasts,

83   CAFs and NAFs, during tumour formation and progression, especially regarding their effects on

84   BCSCs.

85

86   As a preliminary investigation, we aimed to determine the roles of CAFs and NFs during the

87   acquisition of BCSC phenotypes and to explore the similarities and differences between BCSCs

88   that are induced by CAFs and NFs from a functional and observational perspective to lay the

89   foundation for further mechanistic exploration.

Materials and methods

91   1.   Cells and cell culture

92   1.1 CAFs and NFs

93   For the primary culture of CAFs and NFs, tissues were collected from 6 breast cancer patients who

94   underwent complete surgical resection of their tumours at Xuanwu Hospital, Capital Medical

95   University. This study was approved by the appropriate Institutional Review Board and Human

96   Ethics Committee, and all participants were adequately informed before the use of their samples.

97   The donors' clinical information is summarized in Table 1.

98

99   **Table 1 Clinical information of the specimen donors.** Age represents the age of the donor at the

100   time of surgery. The histological type of the tissue was invasive ductal carcinoma (IDC).

101   Oestrogen and progesterone receptor status is indicated as "positive/negative" with the

102   corresponding percentage of positive cells. HER-2 positivity in the tissues was determined by

103   fluorescence in situ hybridization (FISH).

104

105 Paired fibroblasts were isolated from the same patient from corresponding tumour and healthy
106 breast tissues more than 3 cm away from carcinoma. After being harvested, tissues were stored in
107 Dulbecco's modified Eagle's medium (DMEM) (Gibco) supplemented with 1% penicillin-
108 streptomycin (Gibco) and immediately transported on ice to the laboratory. The tissues were
109 mechanically chopped, washed three times with phosphate-buffered saline (PBS) (Gibco) and
110 enzymatically digested with prepared reagents for 9-15 h at 37℃. The reagent mixture used for
111 digesting NFs contained collagenase type I (Sigma) and hyaluronidase (Sigma), whereas that for
112 digesting CAFs contained only collagenase. After the cell suspension was filtered with 100-mesh
113 screens and centrifuged at 1000 rpm for 4 min, the cell pellet was resuspended in the fresh DMEM
114 containing 10% heat-inactivated foetal bovine serum (FBS) (BI). These cells were cultured at 37℃
115 in 5% CO_2 and 95% air, and half of the medium was replaced three times a week. All CAFs and
116 NFs were used in the experiments within 8 passages.

117

118 1.2 Cell lines

119 The human breast cancer cell line MCF-7 was purchased from Cobioer Biosciences Corporation
120 (Nanjing, China) and cultured in DMEM containing 10% FBS at 37℃ in a humidified atmosphere
121 of 5% CO_2 and 95% air.

122

123 1.3 Mammosphere culture and dissociation

124 In a published report (Shaw et al. 2012), MCF-7 cells had the highest mammosphere-forming
125 efficiency (MFE) among all kinds of breast cancer cell lines. Thus, we used the mammosphere-
126 forming capacity of cell lines derived from MCF-7 cells to purify and collect BCSCs. MCF-7 cells
127 were cultured to 70–80% confluency and suspended in DMEM/F12 (Gibco) containing 2% B27
128 (Gibco), 20 ng/mL epidermal growth factor (EGF) (Gibco) and 20 ng/ml recombinant basic
129 fibroblast growth factor (bFGF) (PeproTech) to form single cell suspensions. The cell suspensions
130 were plated at a density of 2.5×10^5 cells/10-cm diameter dish with 10 ml culture medium. The
131 cells were incubated in a humidified atmosphere at 37°C and 5% CO_2 for 7 days without moving
132 or disturbing the plates and without replenishing the medium. After a week, "primary
133 mammospheres" were obtained, which were then collected by gentle centrifugation (580 g, 4 min)
134 and trypsinized with 0.05% trypsin/0.53 mM EDTA-4Na (Gibco). To ensure single cell
135 suspension, the cells were passed three times through a 25 G needle on a syringe and inspected
136 under a microscope. The "secondary mammospheres" were plated at the same seeding density and
137 incubated under the same conditions that were used for the generation of primary mammospheres.

138

139   2.   Immunocytochemistry

140   CAFs and NFs were cultured on coverslips at 50-60% confluency. Then, the fibroblasts were fixed

141   in cold acetone for 7 min and incubated overnight with a primary antibody against α-SMA (1:100)

142   (Abcam) at 4℃ in a moist chamber. PBS was used as a control. After being washed three times

143   with PBS, all coverslips were incubated with a peroxidase-conjugated secondary antibody for 15

144   min at room temperature, followed by incubation with 3,3'-diaminobenzidine (DAB). The

145   coverslips with cells were then counterstained with haematoxylin for 2 min and placed on slides.

146

147   3.   Immunohistochemical staining

148   Samples collected from the patients described above were fixed in formalin and embedded in

149   paraffin. Then, the samples were cut into 4-μm sections with a microtome. All sections were air-

150   dried overnight, dewaxed in xylene and dehydrated in alcohol before staining. The primary

151   antibody against α-SMA was the same as that described above. Staining was performed according

152   to the manufacturer's instructions. Antigen retrieval was performed by pressure cooking the

153   sections for 1 min in EDTA.

154

155   4.   Preparation of conditioned medium

156   CAFs and NFs were cultured to 70-80% confluency and were then washed with PBS. After that,

157   cells were cultured in DMEM/F12 or DMEM with neither FBS nor other growth factors for 24 h.

158   The two types of media were pipetted into a centrifuge tube and centrifuged at 1,000 rpm for 5

159   min, and the supernatant was collected and stored at -20℃ in small aliquots to avoid repeated

160   freeze-thaw cycles. Before use, 10% FBS was added to the DMEM supernatant to form CM for

161   the MCF7 cell invasion assay. Similarly, EGF, bFGF and B27 were added to the DMEM/F12

162   supernatant to form CM for BCSC-related experiments.

163

164   5.   Cell invasion assay

165   Invasion assays were conducted using 8-μm-pore Transwell inserts in 24-well plates (Corning).

166   We added 25 μl of growth factor-reduced phenol red-free Matrigel (BD), which was diluted in a

167   1:4 ratio with DMEM, to Transwell inserts on ice and incubated the inserts at 37℃ without

168   disturbance. After 2 h, 3×10^4 MCF-7 cells in 100 μl FBS-free DMEM were seeded in the upper

169   chamber. The plates were divided into the following three groups: a group with CM-derived from

170 CAFs with 10% FBS (CM-CAFs), a group with CM-derived from NFs with 10% FBS (CM-NFs)

171 and a control group with DMEM and 10% FBS. After 48 h of incubation at 37℃ and 5% CO_2, the

172 cells remaining in the upper chambers were removed with a cotton swab, and the inserts were fixed

173 in cold 4% formaldehyde for 5 min and stained with 5% crystal violet for 5 min. Then, the cells

174 that had invaded to the lower surface of the membranes were counted from 6 random fields of

175 views with an inverted microscope at 400× magnification. The assay was performed in triplicate.

176

177 6. Protein analysis

178 6.1 Sample preparation

179 Proteins in culture supernatants were purified using an acetone precipitation method. For whole-

180 cell extractions, cell pellets were lysed with urea-containing lysis buffer (8 M urea and 100 mM

181 Tris-HCl pH 8.0). Protease inhibitors (Pierce™, Thermo Fisher Scientific) were added to protect

182 proteins from degradation, and protein concentrations were measured using the Bradford assay

183 (Eppendorf BioSpectrometer).

184

185 6.2 Trypsin digestion of proteins

186 For whole-cell proteome analyses, proteins were digested using the filter assisted sample

187 preparation (FASP) method as follows: the protein samples were incubated with 1 M dithiothreitol

188 (DTT) at a final concentration of 5 mM for 30 min at 56°C; then, iodoacetamide (IAA) was added

189 to the samples at a final concentration of 20 mM and incubated in the dark at room temperature.

190 After incubation for half an hour, the samples were mixed with DTT at a final concentration of 5

191 mM and kept in the dark for another 15 min. Then, the protein samples were loaded onto 10-kD

192 Microcon filtration devices (Millipore) and centrifuged at 12,000 g for 20 min and washed twice

193 with urea-containing lysis buffer (8 M urea and 100 mM Tris-HCl pH 8.0) and twice with 50 mM

194 NH_4HCO_3. Then, the samples were digested using trypsin at an enzyme to protein mass ratio of

195 1:25 overnight at 37°C. Peptides were then extracted and dried (SpeedVac, Eppendorf).

196

197 6.3 Mass spectrometric analysis and data processing

198 Orbitrap Fusion liquid chromatography and tandem mass spectrometry (LC-MS/MS) analyses

199 were performed on an Easy-n LC 1000 liquid chromatography system (Thermo Fisher Scientific)

200 coupled to an Orbitrap Fusion MS and a nano-electrospray ion source (Thermo Fisher Scientific).

201 Samples were dissolved in loading buffer (5% methanol and 0.1% formic acid) and loaded onto a

360-µm ID x 2 cm C18 trap column at a maximum pressure 280 bar with 12 µl solvent A (0.1% formic acid in water). Peptides were separated on a 150-µm ID x 10 cm C18 column (1.9 µm, 120 Å, Dr Maisch GmbH) with a series of adjusted linear gradients according to the hydrophobicity of fractions with a flow rate of 500 nl/min. MS analysis was performed in a data-dependent manner with full scans (m/z 300-1,400) acquired using an Orbitrap Mass Analyser at a mass resolution of 120,000 at an m/z of 200. The top data-dependent speed mode was selected for fragmentation in the human collecting duct (HCD) cell at normalized collision energy of 32%, and then fragment ions were transferred into the ion trap analyser with an automatic gain control (AGC) target of 5 × 10^3 counts and maximum injection time of 35 ms. The dynamic exclusion of previously acquired precursor ions was enabled at 18 s.

Raw data were analysed in the Firmiana data analysis environment for protein identification and label-free quantification using a target-decoy approach to identify peptides and proteins at an FDR < 1% against the human protein RefSeq database (released 2013.07.01). Acetylation (protein N terminus) and oxidation (methionine), carbamidomethylation (cysteine) were set as variable modifications.

7. Sphere formation assay

Fourth and higher generation mammospheres were used for the experiments. Cell suspensions prepared as described above in CM and plated at a density of 500 cells/cm² in ultra-low attachment 6-well plates (2 ml of mammosphere medium per well). The plates were divided into 3 groups based on the medium used, namely, CM-CAFs, CM-NFs and DMEM/F12-control medium. All DMEM/F12-control medium used in mammosphere experiments contains DMEM/F12, EGF, bFGF and B27. After 6 days, we counted the number of mammospheres that were more than 50 µm in diameter and calculated MFE based on the following formula: MFE (%) = (number of mammospheres per well/number of cells seeded per well) × 100. The assay was performed in triplicate.

8. Flow cytometry

CD24, CD44 and ALDH1 expression was analysed in cells harvested from fourth and higher generation mammospheres dissociated after 6 days of culture in CM. After preparing single cell suspensions in PBS, 1 × 10^6 cells were counted and resuspended in staining buffer and incubated for 30 min with anti-CD44 and anti-CD24 antibodies (BD) at the manufacturer's suggested dilutions at 4°C in the dark. The labelled cells were washed and resuspended in PBS on ice.

235   Additionally, 1×10^5 cells from the samples were subjected to the ALDEFLUOR assay
236   (Millipore). All samples were analysed with a flow cytometer (BD). Cells incubated with isotype
237   control antibodies corresponding to each fluorescent probe were used as negative controls. In
238   addition, cells incubated with diethylaminobenzaldehyde (DEAB), an inhibitor of ALDH1, were
239   used as negative controls for the ALDEFLUOR assay. The assay was performed in triplicate.

240

241   9.   Immunofluorescence staining

242   For immunofluorescence, mammospheres were cultured on coverslips in CM for 6 days, fixed in
243   cold acetone for 7 min and then stored in PBS. After being washed, the mammospheres were
244   blocked in methanol containing hydrogen peroxide for 10 min. Then, the mammospheres were
245   incubated with primary antibodies (ALDH1A1, Proteintech) (CD44, Cell Signaling) at 4℃
246   overnight in a humid chamber. After being washed 3 times with PBS, the cells were incubated for
247   1 h with secondary antibodies. The coverslips were mounted with mounting medium containing
248   DAPI. Fluorescence signals were observed and images were obtained with a fluorescence
249   microscope. The assay was performed in triplicate.

250

251   10. Statistical analysis

252   Data were presented as the means ± SD for at least three independent experiments for every group.
253   Statistical analyses were performed with SPSS 16.0 software. Statistical differences were analysed
254   using two-tailed Student's t tests. Differences were considered significant at P values less than
255   0.05.

256

257   **Results**

258   CAFs and their paired NFs were successfully isolated from six primary breast cancer samples and
259   paired normal breast tissue specimens, respectively. The primary fibroblasts were successfully
260   cultured in DMEM containing 10% FBS, and these fibroblasts could grow well for at least 9
261   passages. Both CAFs and their paired NFs had similar spindle-like morphology (Fig. 1A-B).
262   Depending on the age of the patients from whom the samples were obtained, senescent cells were
263   observed in different passages, especially after the sixth passage. The cultured CAFs/NFs and
264   breast cancer/adjacent normal tissues all expressed α-SMA, which is considered myofibroblast-
265   specific marker (Fig. 1C-1F). Then, a culture system with CM was established to identify the
266   different roles of CAFs and NFs in the tumour's paracrine microenvironment. In contrast with the

267 cells grown in culture systems with CM-NFs and DMEM with 10%FBS, MCF-7 cells grown in
268 culture systems with CM-CAFs displayed increased invasion (Fig. 1G-I). Therefore, CAFs and
269 NFs could be isolated from different tissues and exerted different functions in the tumour
270 microenvironment.

271

272 **Figure 1**. **Cell morphology and α-SMA expression cannot be used to distinguish CAFs and**
273 **NFs, but these fibroblasts differ in their biological functions.** (A-B) CAFs and NFs are both
274 morphologically characterized as large spindle-shaped cells with indented nuclei. Bar: 100 μm.
275 (C-D) Immunohistochemical staining for α-SMA in CAFs and NFs. Both samples are positive for
276 α-SMA expression. Bar: 100 μm. (E-F) Immunohistochemical staining for α-SMA in a cancer
277 tissue and a paracancerous tissue more than 3 cm away from a carcinoma. Bar: 100 μm. (G-I)
278 Invasion of MCF-7 cells was affected by CM. Bar: 100 μm.

279

280 We collected samples of whole-cell extracts from 6 paired primary fibroblast lines cultured at 90-
281 100% confluence. Label-free LC-MS/MS quantification was used to characterize the differences
282 in protein expression between CAFs and NFs. In total, 7208 proteins were identified. With the
283 criteria of up-regulation in at least 4 paired experiments and a fold-change > 2, 200 proteins were
284 up-regulated in CAFs, and 5037 proteins were up-regulated in NFs. Quantitative data for the
285 proteins up-regulated in CAFs is represented in the form of a heat map (Fig. 2A). The functions,
286 biological processes (Fig. 2B) and Kyoto Encyclopaedia of Genes and Genomes (KEGG)
287 pathways (Fig. 2C) associated with these proteins were also analysed. The proteomic data
288 illustrated differences in protein expression between paired CAFs and NFs.

289

290 **Figure 2 CAFs and NFs are heterogeneous in terms of their protein expression profiles,**
291 **cellular functions and related signalling pathways.** (A) Heterogeneity in the expression of
292 selected proteins (fold-change < -2 or > 2, P < 0.05) between CAFs and NFs. Blue represents
293 down-regulated expression, and red indicates up-regulated expression. All data are transformed by
294 log2 operation. (B) Gene ontology (GO)-based enrichment analysis of up-regulated proteins in
295 CAFs (orange bars) and in paired NFs (blue bars), including cell component (CC), biological
296 process (BP) and molecular function (MF). (C) KEGG pathway analysis for identifying major
297 biological pathways that were different between CAFs (orange bars) and NFs (blue bars).

298

299 To explore the role of CAFs and NFs in BCSCs, we employed a culture system with CM from
300 corresponding fibroblasts and analysed the effect of the CM on mammosphere formation by MCF-
301 7 cells. Single cell suspensions of MCF-7 cells were cultured independently in CM-CAFs, CM-
302 NFs and DMEM/F12-control medium as mentioned above, without disturbing the plates.
303 Mammospheres, with rounded shape and smooth boundaries, were observed by microscopy after
304 6 days of culture (Fig. 3A). Mammospheres greater than 50 μm in diameter were counted and
305 included in statistical analyses. The average size of the mammospheres was not noticeably
306 different among the groups. However, the number of mammospheres formed in the groups with
307 CM-CAFs and CM-NFs was approximately 3.84-fold and 2.85-fold higher, respectively, than that
308 in the control group (Fig. 3B). Cells cultured in CM-CAFs had a greater MFE than the cells
309 cultured in CM-NFs (P<0.05) (Fig. 3C). Thus, CM-CAFs demonstrated greater capability of
310 inducing mammosphere formation than did CM-NFs.

311

312 **Figure 3**. **Mammosphere formation by MCF-7 cells cultured in CM.** (A) Mammosphere
313 formation in MCF-7 cells in the control, CM-NFs (cultured in CM-NFs) and CM-CAFs (cultured
314 in CM-CAFs) groups. Bar: 100 μm. (B) Number of mammospheres greater than 50 μm in diameter
315 in each group. (C) MFE in each group.

316

317 We performed serial flow cytometry to explore the relationship between $CD44^+CD24^-$ and
318 $ALDH1^+$ cell populations, corresponding to the expression of markers that are widely used to
319 characterize BCSCs. Overall, $ALDH1^+$ BCSCs were highly enriched in the CM-CAFs group (Fig.
320 4A-C), whereas cells in the CM-NFs group were enriched for the $CD44^+CD24^-$ population (Fig.
321 4D-F). Based on the ALDEFLUOR assay, the proportion of $ALDH1^+$ cells increased in CM-CAFs
322 relative to those in the groups with both DMEM/F12-control medium and NF-conditioned medium
323 $(P < 0.01)$.

324 However, there was no significant difference in the proportion of the $CD44^+CD24^-$ population
325 between cells cultured CM-CAFs and cells cultured on DMEM/F12-control medium $(P = 0.181)$,
326 but the proportion of $CD44^+CD24^-$ BCSCs was markedly increased among the cells cultured in
327 CM-NFs $(P < 0.05)$.

328

329 **Figure 4 CM from CAFs and NFs can induce phenotypic transition in BCSCs.** (A-C) ALDH1
330 expression in MCF-7 mammospheres from the three groups based on the ALDEFLUOR assay
331 followed by fluorescence activated cell-sorting (FACS). (D-F) CD24 and CD44 expression in

332   MCF-7 mammospheres from the three groups as detected by FACS. (G-H) Localization of CD44
333   (green), ALDH1 (red) and DAPI (blue) in mammospheres adhered to glass slides as assessed by
334   immunofluorescence. Bar: 100 μm.

335

336   Further, the expression of CD44 and ALDH1 was examined using immunofluorescence in the two
337   groups of mammospheres cultured in different CM. The expression of ALDH1 in the cytoplasm
338   was enhanced by paracrine stimulation via CM-CAFs (Fig. 4G). Additionally, the mammospheres
339   displayed significantly enhanced CD44 expression when cultured in CM-NFs (Fig. 4H).

340

Discussion

341

342   In the present study, we used proteomics methods to investigate the protein profiling of breast
343   cancer CAFs and their normal counterpart NFs, which were isolated from breast cancer and paired
344   with paracancerous tissues. We found that the differences in expression patterns between CAFs
345   and NFs were mainly focused on the regulation of cellular extracellular matrix remodelling,
346   metabolism and regulation of TGF-β pathways. We also found that the CM from CAFs and NFs
347   has different biological functions in promoting the invasiveness of breast cancer cells, consistent
348   with previous reports (Chen et al. 2012). Interestingly, our work demonstrated that the CM from
349   both CAFs and NFs could increase the MFE of MCF-7 cells. Compared with the CM from CAFs,
350   the CM from NFs could induce an increase in the proportion of CD44$^+$CD24$^-$ BCSCs. Considering
351   that the evidence-based data, which illustrates the effect of fibroblasts on the phenotypic
352   transformation of BCSCs to various states, are limited and tend to rely on studies focusing on
353   CAFs (Gunaydin et al. 2013; Lisanti et al. 2014), the present study might broaden our horizons of
354   the critical roles of both CAFs and NFs in the dedifferentiation and phenotype conversion of breast
355   cancer cells.

356

357   Though several studies have already reported several classic biomarkers for CAFs, few of them
358   are proved to be specific, such as α-SMA (Qiao et al. 2016). In this study, immunohistochemical
359   (IHC) staining was applied to detect the expression levels of α-SMA in paraffin-embedded breast
360   cancer tissues and para-carcinoma tissues and in isolated CAFs/NFs, and we found that both CAFs
361   and NFs expressed α-SMA, as observed in previous studies (Huang, Li et al. 2010), despite some
362   differences in staining patterns. This finding drives us to conduct a systemic evaluation of protein
363   expression between CAFs and NFs. Heat map cluster analysis demonstrated the differences
364   between the protein expression profiles of these two fibroblast types, which were consistent with

365 previously reported GeneChip data (Al-Rakan et al. 2013; Pasanen et al. 2016). Furthermore, GO
366 analysis revealed that compared to the proteins up-regulated in NFs, the proteins up-regulated in
367 CAFs were associated with cytoskeleton formation, cell adhesion and integrin-mediated signalling
368 pathways. Moreover, the identified proteins regulate the TGF-β signal pathway. However, the
369 proteins down-regulated in CAFs were associated with gene transcription and translation,
370 lysosome transport, oxidative stress, mitochondria and cell morphology, among other processes.
371 KEGG analysis showed that the pathways up-regulated in CAFs were associated with intercellular
372 adhesion and connection. These pathways can also regulate the formation of the cytoskeleton. The
373 pathways down-regulated in CAFs were associated with RNA degradation, RNA transport and
374 fatty acid metabolism. Our data provide a comprehensive view of the protein profiling of CAFs
375 and NFs, which might provide valuable biomarkers for CAFs. In fact, data mining and validation
376 to identify intracellular and secreted extracellular protein expression profiles in CAFs and NFs are
377 ongoing.

378

379 There is a consensus that CAFs can affect the invasive behaviour of breast cancer cells (Luo et al.
380 2015). However, the underlying mechanism of how CAFs affect the invasive potential of breast
381 cancers is still uncertain. In the present study, we proved that the CM from CAFs could promote
382 the invasiveness of the breast cancer cell line MCF-7, which could be explained by our proteomic
383 results that the well-known TGF-β oncogenic signalling pathway was significantly up-regulated
384 in CAFs. We hypothesized that CAFs could enhance the metastatic potential of breast cancer cells
385 though the paracrine stimulation of TGF-β. In fact, there have been reports of TGF-β supported
386 tumour invasion by several mechanisms, for example, stimulating the trans-differentiation of
387 epithelial cancer cells into migratory mesenchymal cells, namely the epithelial-mesenchymal
388 transition (EMT) process (Yu et al. 2014). In addition, in some human breast cancer cells,
389 organization of the invadopodia or degradation of the ECM requires extracellular or intracellular
390 signal-regulated kinase signalling through phosphatidylinositide 3-kinase and Src kinase, which is
391 also governed by TGF-β (Mandal et al. 2008; Pignatelli et al. 2012). In our subsequent work, we
392 will investigate whether TGF-β signalling contributes to CAF-induced acquisition of invasion
393 potential in breast cancer cells. Moreover, details of the mechanism will be illustrated.

394

395 The highlight in our study is that we clarified the roles of CAFs and NFs in the induction of cancer
396 stem cells. Compared with the DMEM/F12-control medium, the CM from CAFs and NFs could
397 significantly enhance the MFE of MCF-7 cells. Among the CM from the two kinds of fibroblasts,
398 the mammosphere-promoting effect was stronger for the CM-CAFs. These data are also consistent

399   with the findings of stem cell-related studies in which fibroblasts are used as feeder cells or in co-
400   culture systems cells to maintain the characteristics of stem cells and to induce the dedifferentiation
401   of non-stem cells (Chen et al. 2014; Zhang et al. 2011). Further, using flow cytometry and
402   immunofluorescence, we found that the cytokines or exosomes secreted by CAFs and NFs could
403   induce the phenotypic transformation of BCSCs. ALDH1, CD44 and CD24 are common markers
404   used for the identification of BCSCs. Previous studies on the effects of tumour stroma on BCSCs
405   did not investigate the effect on phenotypic transformation. Liu et al. proposed that although
406   ALDH1$^+$ BCSCs and CD44$^+$CD24$^-$ BCSC are overlapping cell populations, they are not identical
407   (Liu et al. 2014). The former cell population is highly proliferative, while a majority of
408   CD44$^+$CD24$^-$ BCSCs are typically quiescent. A rare proportion of ALDH1$^+$ and CD44$^+$CD24$^-$
409   BCSCs displays very strong tumourigenicity in vivo (Croker et al. 2009). Immunofluorescence
410   assay showed that ALDH1$^+$ BCSCs and CD44$^+$CD24$^-$ BCSCs are localized in different regions
411   within the tumour tissue. The former cell population is typically located in the centre of the tumour,
412   while the latter is located more at the periphery. In this study, the proportion of ALDH1$^+$ BCSCs
413   was relatively increased in response to CM-CAFs; however, BCSCs treated with CM-NFs were
414   more likely to undergo phenotypic transformation into CD44$^+$ populations. Thus, we hypothesized
415   that the effect of fibroblasts on BCSCs may be multidirectional. Fibroblasts at different states may
416   have different effects on BCSC populations and thus promote diverse biological processes. As
417   shown in this study, CM-CAFs could promote the invasion of tumour cells in a paracrine manner,
418   while cytokines secreted by NFs suppressed local invasion of tumour cells. Since accumulating
419   evidence has demonstrated a crucial role of TGF-β in the regulation of cancer stem cell function
420   (Watabe & Miyazono 2009), it has been observed that TGF-β can affect the generation and
421   outcome of normal and malignant stem cells through various mechanisms (Watabe & Miyazono
422   2009). In breast cancer, previous studies have reported that the activation of the TGF-β pathway
423   can enrich CD44$^+$ BCSCs (Shipitsin et al., 2007). However, other groups have also found that
424   active TGF-β signalling can increase a subpopulation of stemness cells that express ALDH1
425   (Zheng R 2014), suggesting that the regulatory function of TGF-β in BCSCs is complicated. In
426   our present work, we found that TGF-β activated fibroblasts, namely the CAFs, could increase the
427   proportion of ALDH1$^+$ BCSCs via their conditioned medium. These results hinted that TGF-β as
428   a paracrine factor might be effective as a regulator in the transformation of BCSC subpopulations
429   from CD44$^+$ to ALDH1$^+$. This study expanded on the conclusion that fibroblasts can promote the
430   generation of cancer stem cells. Further, we will study whether such a subpopulation conversion
431   is associated with tumour progression, such as tumour invasion, and the underlying mechanism of
432   this process.

433

434   This study has some potential limitations. First, although in vivo experiments are the gold standard
435   for verifying the self-renewal ability of cancer stem cells, we cannot prevent phenotypic changes
436   induced by tumour cells in NFs in vivo. We do not have data from in vivo experiments
437   investigating the effects of NFs and CAFs on cancer stem cells. In addition, this research only
438   proves that CM from CAFs or NFs enrich the BCSCs, however future study is needed to find out
439   the exact approach that induces this promoting effect. It may the result of increased proliferation
440   of BCSCs, represent of low apoptosis ration, or the conversion of non-stem cells into stem cells.
441   At last, because this study is preliminary, the results merely describe the effect of CAFs/NFs on
442   the phenotype of BCSCs from a functional perspective. Further molecular analyses are needed to
443   explore the associated cytokines or pathways, and we will pursue this direction in the future.

444

Conclusions

446   In summary, our preliminary study validated the existence of heterogeneity among CAFs and NFs
447   from a proteomics perspective. Both types of fibroblasts promoted the self-renewal capacity of
448   BCSCs and induced the phenotypic transformation of non-stem cells to cancer stem cells.
449   However, during this process, CAFs and NFs showed different extents of promotive ability and
450   different directions of phenotypic transformation in BCSCs. Further investigation on the effect of
451   NFs on cancer stem cells may provide a new direction for the elucidation of the initial stages of
452   tumour metastasis. Additionally, insights into the effects of CAFs/NFs on BCSCs may provide
453   new directions in the study of breast cancer treatment. Based on the functional evidence obtained
454   in this study, further studies will be carried out to explore the molecular mechanisms and relative
455   pathways involved in the phenotypic transformation of BCSCs.

456

Acknowledgements

458   We thank Prof Jun Qin, Ph.D., State Key Laboratory of Proteomics, National Center for Protein
459   Sciences, Beijing Proteome Research Center, Yeqing Cui, medical laboratory technician of
460   Xuanwu Hospital Surgery Lab, Jiaying Yu, Ph.D., Institute of Biophysics, Chinese Academy of
461   Sciences, for their expertise and help during this project, and Dr Tian Lan, Dr Ye Cheng and Dr
462   Fei Gao for proofreading and language check.

463

References

465 A DACP, and Lopes C. 2017. Implications of Different Cancer Stem Cell Phenotypes in Breast Cancer. *Anticancer*
466   *Res* 37:2173-2183. 10.21873/anticanres.11552

467 Al-Hajj M, Wicha MS, Benito-Hernandez A, Morrison SJ, and Clarke MF. 2003. Prospective identification of
468   tumorigenic breast cancer cells. *Proc Natl Acad Sci U S A* 100:3983-3988. 10.1073/pnas.0530291100

469 Al-Rakan MA, Colak D, Hendrayani SF, Al-Bakheet A, Al-Mohanna FH, Kaya N, Al-Malik O, and Aboussekhra A.
470   2013. Breast stromal fibroblasts from histologically normal surgical margins are pro-carcinogenic. *J Pathol*
471   231:457-465. 10.1002/path.4256

472 Bernardi MA, Logullo AF, Pasini FS, Nonogaki S, Blumke C, Soares FA, and Brentani MM. 2012. Prognostic
473   significance of CD24 and claudin-7 immunoexpression in ductal invasive breast cancer. *Oncol Rep* 27:28-
474   38. 10.3892/or.2011.1477

475 Boesch M, Sopper S, Zeimet AG, Reimer D, Gastl G, Ludewig B, and Wolf D. 2016. Heterogeneity of Cancer Stem
476   Cells: Rationale for Targeting the Stem Cell Niche. *Biochim Biophys Acta* 1866:276-289.
477   10.1016/j.bbcan.2016.10.003

478 Buchsbaum RJ, and Oh SY. 2016. Breast Cancer-Associated Fibroblasts: Where We Are and Where We Need to
479   Go. *Cancers (Basel)* 8. 10.3390/cancers8020019

480 Bussard KM, Mutkus L, Stumpf K, Gomez-Manzano C, and Marini FC. 2016. Tumor-associated stromal cells as
481   key contributors to the tumor microenvironment. *Breast Cancer Res* 18:84. 10.1186/s13058-016-0740-2

482 Chen P, Mo Q, Wang B, Weng D, Wu P, and Chen G. 2012. Breast cancer associated fibroblasts promote MCF-7
483   invasion in vitro by secretion of HGF. *J Huazhong Univ Sci Technolog Med Sci* 32:92-96. 10.1007/s11596-
484   012-0016-8

485 Chen WJ, Ho CC, Chang YL, Chen HY, Lin CA, Ling TY, Yu SL, Yuan SS, Chen YJ, Lin CY, Pan SH, Chou HY,
486   Chen YJ, Chang GC, Chu WC, Lee YM, Lee JY, Lee PJ, Li KC, Chen HW, and Yang PC. 2014. Cancer-
487   associated fibroblasts regulate the plasticity of lung cancer stemness via paracrine signalling. *Nat Commun*
488   5:3472. 10.1038/ncomms4472

489 Chiotaki R, Polioudaki H, and Theodoropoulos PA. 2016. Stem cell technology in breast cancer: current status and
490   potential applications. *Stem Cells Cloning* 9:17-29. 10.2147/SCCAA.S72836

491 Croker AK, Goodale D, Chu J, Postenka C, Hedley BD, Hess DA, and Allan AL. 2009. High aldehyde
492   dehydrogenase and expression of cancer stem cell markers selects for breast cancer cells with enhanced
493   malignant and metastatic ability. *J Cell Mol Med* 13:2236-2252. 10.1111/j.1582-4934.2008.00455.x

494 Darby IA, Zakuan N, Billet F, and Desmouliere A. 2016. The myofibroblast, a key cell in normal and pathological
495   tissue repair. *Cell Mol Life Sci* 73:1145-1157. 10.1007/s00018-015-2110-0

496 Erdogan B, and Webb DJ. 2017. Cancer-associated fibroblasts modulate growth factor signaling and extracellular
497   matrix remodeling to regulate tumor metastasis. *Biochem Soc Trans* 45:229-236. 10.1042/BST20160387

498 Giannoni E, Bianchini F, Masieri L, Serni S, Torre E, Calorini L, and Chiarugi P. 2010. Reciprocal activation of
499   prostate cancer cells and cancer-associated fibroblasts stimulates epithelial-mesenchymal transition and
500   cancer stemness. *Cancer Res* 70:6945-6956. 10.1158/0008-5472.CAN-10-0785

501 Ginestier C, Hur MH, Charafe-Jauffret E, Monville F, Dutcher J, Brown M, Jacquemier J, Viens P, Kleer CG, Liu S,
502   Schott A, Hayes D, Birnbaum D, Wicha MS, and Dontu G. 2007. ALDH1 is a marker of normal and
503   malignant human mammary stem cells and a predictor of poor clinical outcome. *Cell Stem Cell* 1:555-567.
504   10.1016/j.stem.2007.08.014

505 Gunaydin G, Dolen Y, and Kesikli SA. 2013. Fibroblast-derived CCL2 induces cancer stem cells--letter. *Cancer Res*
506   73:1031. 10.1158/0008-5472.CAN-12-2379

507 Li X, Lewis MT, Huang J, Gutierrez C, Osborne CK, Wu MF, Hilsenbeck SG, Pavlick A, Zhang X, Chamness GC,
508   Wong H, Rosen J, and Chang JC. 2008. Intrinsic resistance of tumorigenic breast cancer cells to
509   chemotherapy. *J Natl Cancer Inst* 100:672-679. 10.1093/jnci/djn123

510 Lisanti MP, Tsirigos A, Pavlides S, Reeves KJ, Peiris-Pages M, Chadwick AL, Sanchez-Alvarez R, Lamb R,
511   Howell A, Martinez-Outschoorn UE, and Sotgia F. 2014. JNK1 stress signaling is hyper-activated in high
512   breast density and the tumor stroma: connecting fibrosis, inflammation, and stemness for cancer
513   prevention. *Cell Cycle* 13:580-599. 10.4161/cc.27379

514 Liu S, Cong Y, Wang D, Sun Y, Deng L, Liu Y, Martin-Trevino R, Shang L, McDermott SP, Landis MD, Hong S,
515   Adams A, D'Angelo R, Ginestier C, Charafe-Jauffret E, Clouthier SG, Birnbaum D, Wong ST, Zhan M,
516   Chang JC, and Wicha MS. 2014. Breast cancer stem cells transition between epithelial and mesenchymal
517   states reflective of their normal counterparts. *Stem Cell Reports* 2:78-91. 10.1016/j.stemcr.2013.11.009

518 Luo H, Tu G, Liu Z, and Liu M. 2015. Cancer-associated fibroblasts: a multifaceted driver of breast cancer
519   progression. *Cancer Lett* 361:155-163. 10.1016/j.canlet.2015.02.018

520 Mandal S, Johnson KR, and Wheelock MJ. 2008. TGF-beta induces formation of F-actin cores and matrix
521   degradation in human breast cancer cells via distinct signaling pathways. *Exp Cell Res* 314:3478-3493.
522   10.1016/j.yexcr.2008.09.013

523 Mansour SF, and Atwa MM. 2015. Clinicopathological Significance of CD133 and ALDH1 Cancer Stem Cell
524   Marker Expression in Invasive Ductal Breast Carcinoma. *Asian Pacific Journal of Cancer Prevention*
525   16:7491-7496. 10.7314/apjcp.2015.16.17.7491

526 Pasanen I, Lehtonen S, Sormunen R, Skarp S, Lehtilahti E, Pietila M, Sequeiros RB, Lehenkari P, and Kuvaja P.
527   2016. Breast cancer carcinoma-associated fibroblasts differ from breast fibroblasts in immunological and
528   extracellular matrix regulating pathways. *Exp Cell Res* 344:53-66. 10.1016/j.yexcr.2016.04.016

529 Pignatelli J, Tumbarello DA, Schmidt RP, and Turner CE. 2012. Hic-5 promotes invadopodia formation and
530   invasion during TGF-beta-induced epithelial-mesenchymal transition. *J Cell Biol* 197:421-437.
531   10.1083/jcb.201108143

532 Plaks V, Kong N, and Werb Z. 2015. The cancer stem cell niche: how essential is the niche in regulating stemness of
533   tumor cells? *Cell Stem Cell* 16:225-238. 10.1016/j.stem.2015.02.015

534 Qiao A, Gu F, Guo X, Zhang X, and Fu L. 2016. Breast cancer-associated fibroblasts: their roles in tumor initiation,
535   progression and clinical applications. *Front Med* 10:33-40. 10.1007/s11684-016-0431-5

536 Shaw FL, Harrison H, Spence K, Ablett MP, Simoes BM, Farnie G, and Clarke RB. 2012. A detailed mammosphere

537   assay protocol for the quantification of breast stem cell activity. *J Mammary Gland Biol Neoplasia* 17:111-

538   117. 10.1007/s10911-012-9255-3

539 Somasundaram V, Hemalatha SK, Pal K, Sinha S, Nair AS, Mukhopadhyay D, and Srinivas P. 2016. Selective mode

540   of action of plumbagin through BRCA1 deficient breast cancer stem cells. *BMC Cancer* 16:336.

541   10.1186/s12885-016-2372-4

542 Watabe T, and Miyazono K. 2009. Roles of TGF-beta family signaling in stem cell renewal and differentiation. *Cell*

543   *Res* 19:103-115. 10.1038/cr.2008.323

544 Yang F, Xu J, Tang L, and Guan X. 2017. Breast cancer stem cell: the roles and therapeutic implications. *Cell Mol*

545   *Life Sci* 74:951-966. 10.1007/s00018-016-2334-7

546 Yu Y, Xiao CH, Tan LD, Wang QS, Li XQ, and Feng YM. 2014. Cancer-associated fibroblasts induce epithelial-

547   mesenchymal transition of breast cancer cells through paracrine TGF-beta signalling. *Br J Cancer* 110:724-

548   732. 10.1038/bjc.2013.768

549 Zhang F, Song C, Ma Y, Tang L, Xu Y, and Wang H. 2011. Effect of fibroblasts on breast cancer cell

550   mammosphere formation and regulation of stem cell-related gene expression. *Int J Mol Med* 28:365-371.

551   10.3892/ijmm.2011.700

552 Zheng R WJ, Wu Q, Wang Z, Ou Y, Ma L, Wang M, Wang J, Yang Y. 2014. Expression of ALDH1 and TGFβ2 in

553   benign and malignant breast tumors and their prognostic implications. *Int J Clin Exp Pathol* 7:4173-4183.

554

Clinical information of the specimen donors.

Age represents the age of the donor at the time of surgery. The histological type of the tissue was invasive ductal carcinoma (IDC). Oestrogen and progesterone receptor status is indicated as "positive/negative" with the corresponding percentage of positive cells. HER-2 positivity in the tissues was determined by fluorescence in situ hybridization (FISH).

Sample name	Patient' age	Histological type	Largest diameter	ER	PR	HER-2	Ki67	Axillary lymph node metastasis	Cyclomastopathy
CAF-g/ NF-g	46	IDC	25 mm	+, 80 %	+, 40%	Negative	15%	Yes	Yes
CAF-h/ NF-h	33	IDC	33 mm	+, 95 %	+, 10%	Negative	20%	Yes	Yes
CAF-i/ NF-i	60	IDC	18 mm	+, 95 %	+, 80%	Positive	5%	No	Yes
CAF-l/NF-l	44	IDC	26 mm	+, 80 %	-	Negative	25%	Yes	Yes
CAF-m/NF-m	47	IDC	30 mm	+, 95 %	+, 90%	Negative	15%	Yes	Yes
CAF-n/NF-n	66	IDC	30 mm	+, 95 %	-	Negative	30%	Yes	Yes

Table 1 Clinical information of the specimen donors. Age represents the age of the donor at the time of surgery. The histological type of the tissue was invasive ductal carcinoma (IDC). Oestrogen and progesterone receptor status is indicated as "positive/negative" with the corresponding percentage of positive cells. HER-2 positivity in the tissues was determined by fluorescence in situ hybridization (FISH).

Figure 1

Cell morphology and α-SMA expression cannot be used to distinguish CAFs and NFs, but these fibroblasts differ in their biological functions.

(A-B) CAFs and NFs are both morphologically characterized as large spindle-shaped cells with indented nuclei. Bar: 100 μm. (C-D) Immunohistochemical staining for α-SMA in CAFs and NFs. Both samples are positive for α-SMA expression. Bar: 100 μm. (E-F) Immunohistochemical staining for α-SMA in a cancer tissue and a paracancerous tissue more than 3 cm away from carcinoma. Bar: 100 μm. (G-I) Invasion of MCF-7 cells was affected by CM. Bar: 100 μm.
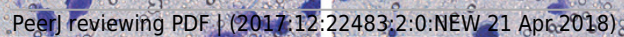
Figure 2

CAFs and NFs are heterogeneous in terms of their protein expression profiles, cellular functions and related signalling pathways.

(A) Heterogeneity in the expression of selected proteins (fold-change < -2 or > 2, P < 0.05) between CAFs and NFs. Blue represents down-regulated expression, and red indicates up-regulated expression. All data are transformed by log2 operation. (B) Gene ontology (GO)-based enrichment analysis of up-regulated proteins in CAFs (orange bars) and in paired NFs (blue bars), including cell component (CC), biological process (BP) and molecular function (MF). (C) KEGG pathway analysis for identifying major biological pathways that were different between CAFs (orange bars) and NFs (blue bars).

A

B

C
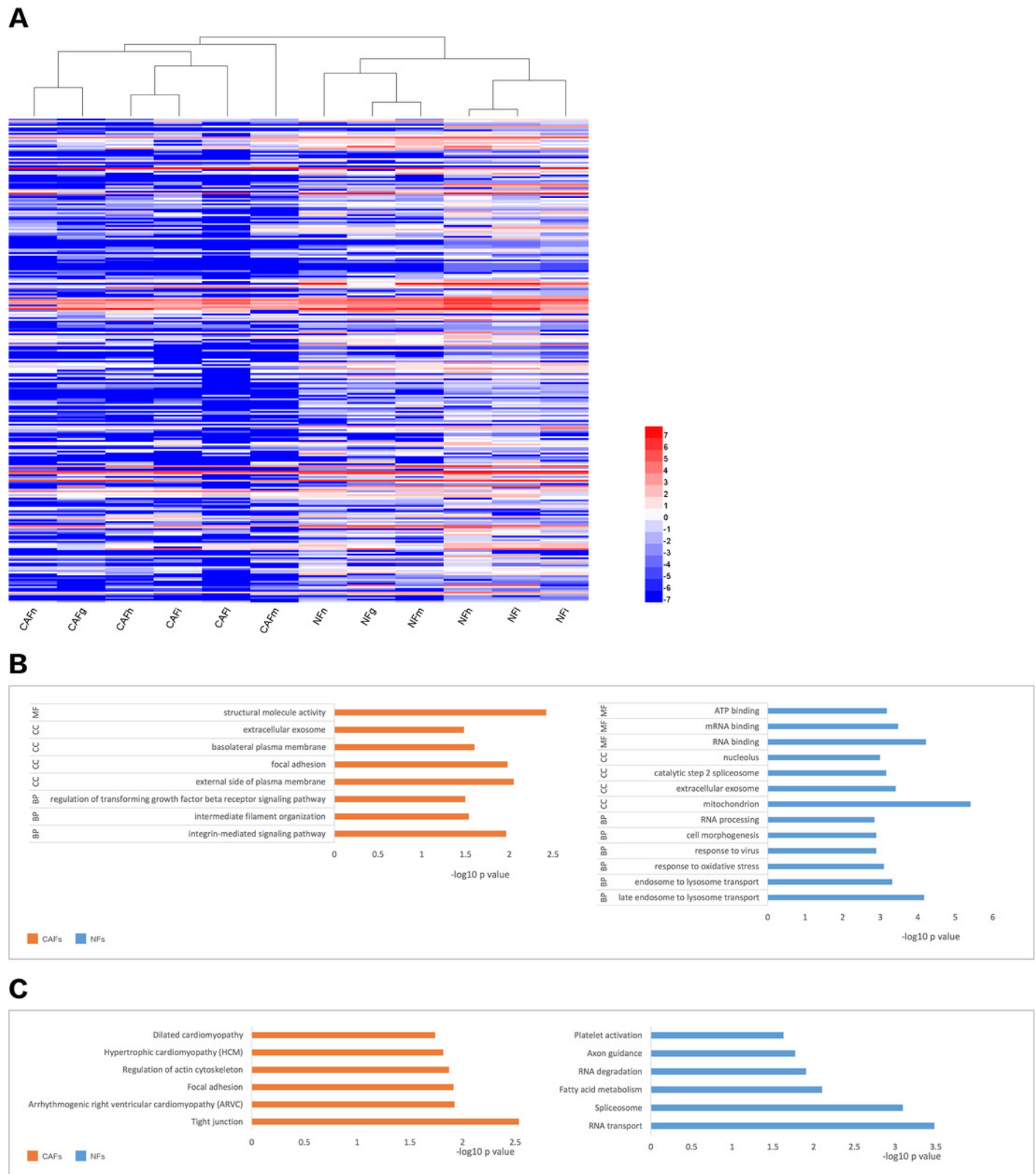
Figure 3

Mammosphere formation by MCF-7 cells cultured in CM.

(A) Mammosphere formation in MCF-7 cells in the control, CM-NFs (cultured in CM-NFs) and CM-CAFs (cultured in CM-CAFs) groups. Bar: 100 μm. (B) Number of mammospheres greater than 50 μm in diameter in each group. (C) MFE in each group.
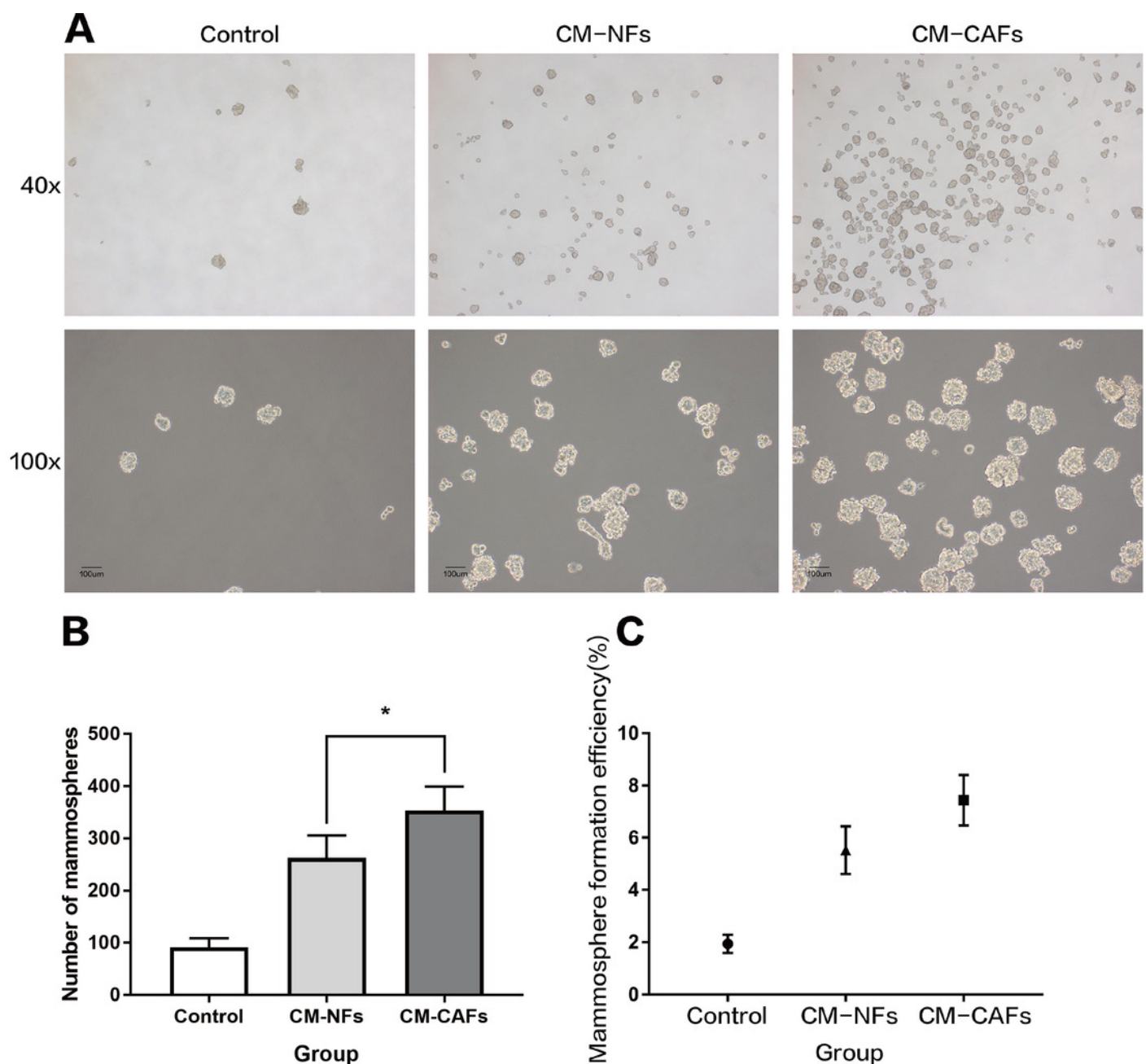
Figure 4

CM from CAFs and NFs can induce phenotypic transition in BCSCs.

(A-C) ALDH1 expression in MCF-7 mammospheres from the three groups based on the ALDEFLUOR assay followed by fluorescence activated cell-sorting (FACS). (D-F) CD24 and CD44 expression in MCF-7 mammospheres from the three groups as detected by FACS. (G-H) Localization of CD44 (green), ALDH1 (red) and DAPI (blue) in mammospheres adhered to glass slides as assessed by immunofluorescence. Bar: 100 μm.

A Control

B CM−NFs

C CM−CAFs

0.29 ± 0.13%

0.71 ± 0.46%

2.04 ± 0.71%

D Control

E CM−NFs

F CM−CAFs

9.77 ± 5.15%

22.41 ± 7.01%

13.79 ± 3.14%

G

H

CM−CAFs

CM−NFs